Journal of Applied Electrochemistry **34**: 891–897, 2004.
© 2004 *Kluwer Academic Publishers. Printed in the Netherlands.*

Corrosion protection of mild steel by formation of iron oxide polybithiophene composite films

S.A.M. REFAEY*, F. TAHA and H.S. SHEHATA
Department of Chemistry, Faculty of Science, Minia University, Minia, Egypt
*(*author for correspondence, e-mail: saeed_refaey@hotmail.com)*

Received 20 November 2002; accepted in revised form 24 March 2004

Key words: cyclic voltammetry, electropolymerization, mild steel, platinum, polythionphene

Abstract

Polybithiophene (PBT) was freshly electrodeposited on platinum (Pt) and steel electrodes using cyclic voltammetry from 2,2′-bithiophene (BT), electrolyte and acetonitrile (AC). The electrolytes used were $LiBF_4$, $LiClO_4$, $LiCF_3SO_3$, Bu_4NBF_4, Bu_4NClO_4, or $Bu_4NCF_3SO_3$. Black to red colored PBT films with metallic lustre were electropolymerized on Pt and steel electrodes with good adherence. The electrochemical properties and the surface morphology of the deposited PBT film depend on the type of ions used during the electropolymerization. It was found that the steel surface was covered with Fe_xO_y–PBT composite. The results are discussed on the basis of the structural and the electrochemical properties of the electrolyte ions. The presence of PBT–iron oxide composite on the steel surface causes a shift of the pitting potential (E_{pit}) in the positive direction, indicating the inhibitive effect of PBT–Fe_xO_y composite on the chloride pitting corrosion.

1. Introduction

Electrochemical polymerization has proved a useful method of obtaining conjugated aromatic polymers, e.g. polypyrrole [1] and polythiophene [2]. Conductive polymers have been candidates for corrosion protection [3–7]. Contradictory results can be found concerning the possibility of electrodeposition of polyaniline and the effects of this polymer on the corrosion resistance of iron [8]. An interesting compound for this purpose is the BT, since it can form adherent and high conductivity polymer films. The BT has a low electropolymerization potential (1320 mV) relative to thiophene itself (2060 mV) [9]. Moreover, it has a medium polymerization potential, which prevents the oxidation of the substrate during the electropolymerization. The produced PBT has a low oxidation potential (1000 mV) relative to water oxidation (1200 mV) [10]. This is an advantage in industrial applications, especially in aqueous solutions. In order to obtain the best PBT film, the effect of different electrolyte anions and cations used during electropolymerization on the quality of the PBT film formed on the steel surface was examined. High quality implies an adhesive, non-porous (to impede the migration of aggressive ions to the underlying steel surface) and homogeneous with metal oxide film formed (as composite). This paper discusses the electrodeposition of high quality PBT film on steel surfaces and the influence of aggressive ions (as Cl^- ions) on the PBT–Fe_xO_y protective film.

2. Experimental

The BT monomer (Aldrich) was used as received. The solutions were prepared from spectrograde acetonitrile (AC). All electrolytes (Fluka), $LiBF_4$, $LiClO_4$, $LiCF_3SO_3$, Bu_4NBF_4, Bu_4NClO_4, and $Bu_4NCF_3SO_3$, were analytical grade. The PBT films were synthesized by electrochemical oxidation of BT in a three-electrode cell. The working electrode was made from Pt (treated as described previously [11]) or steel. The steel working electrode was produced in the electric arc furnace of the Delta Steel Mill Company, Cairo. The composition (wt%) was 0.16% C, 1.0 Mn, 0.45 S, 0.30 P, 0.20 Si and 0.08 V. The ingots were hot rolled (at 1000–1200 °C) and then machined in the form of short rods (hot rolled electrodes), each 27 mm in length and 8 mm in diameter. Each working electrode was constructed and treated following the procedure described previously [12, 13]. A Pt wire was used as a counter electrode and silver/silver chloride as reference. The solutions used for electropolymerization contained 0.05 M BT and 0.1 M electrolyte in acetonitrile; it was deaerated by nitrogen bubbling. The polymer films were deposited by cyclic voltammetry between −500 and 1600 mV (one cycle). The cyclic voltammetry curves were run on a potentiostat (AMEL model 2049), which was PC-controlled. All experiments were carried out at room temperature (25 °C). The morphology of the PBT surface formed on the Pt electrode was examined by SEM (CamScan Cambridge Scanning) and the PBT surface formed on

the steel electrode was examined by a SEM (Jeol JSM T200).

3. Results and discussion

3.1. *Electropolymerization of 2,2′-bithiophene on platinum*

The cyclic voltammetry curves of the electrodpolymerization of 2,2′-bithiophene (BT) on Pt in the potential range −500 to 1600 mV in the presence of either, $LiBF_4$, $LiClO_4$, $LiCF_3SO_3$, Bu_4NBF_4, Bu_4NClO_4 or $Bu_4NCF_3SO_3$ were investigated. In all cases, the curves have the same general feature (Figure 1a and b). The numbers labeling the curves in all figures indicate the number of the cycle. The anodic potential peak (E_{ap}) of the anodic oxidation of the BT are 1310, 1320, 1330, 1350, 1360 and 1330 mV for $LiBF_4$, $LiClO_4$, $LiCF_3SO_3$, Bu_4NBF_4, Bu_4NClO_4, and $Bu_4NCF_3SO_3$ respectively. The BT undergoes oxidation and subsequent electropolymerization at potentials more positive than 700 mV [14]. The PBT films are formed by the following processes: (1) electroinitiation (in which the transfer of electron occurs between the electrode and any one non-polymerizable electroactive substance, which acts as electrochemical activator), (2) nucleation, (3) propagation and (4) formation of the polymer film [15]. The area under the anodic curve is proportional to the number of oxidized sites in the film. Increase in the cycle number leads to a decrease in the anodic current peak, where at low concentrations of BT, the PBT formed in the 1st anodic span is overoxidizing at 1200 mV [16, 17]. The overoxidized PBT film forms an insulator layer, which impedes diffusion of the BT species to the Pt surface. The anodic potential peak is shifted in the positive direction with increase in cycle number. This result may be interpreted in terms of the deactivation of the PBT formed in successive cycles by incorporation of the bulky anions and/or cations [11], which are able to localize the polarons of the PBT film like $CF_3SO_3^-$ and/or Bu_4N^+. Similar results (incorporation of anions and cations in the polymer) were described [6] for polypyrrole by the using quartz crystal microbalance technique. It was shown that cation and anion exchange takes place simultaneously and that, in the case of strongly bound anions (as $CF_3SO_3^-$), cation exchange is predominant. Genies and Pernaut [7] suggested that the dissolved salt (cation and anion) is incorporated into the polypyrrole film during the doping step. The relations between the charge consumed (Q_c) and the potential during the electropolymerization of BT on the Pt surface in the presence of different electrolytes ($LiBF_4$, $LiClO_4$, $LiCF_3SO_3$, Bu_4NBF_4, Bu_4NClO_4, and $Bu_4NCF_3SO_3$) are shown in Figure 2 (as example). At potentials lower

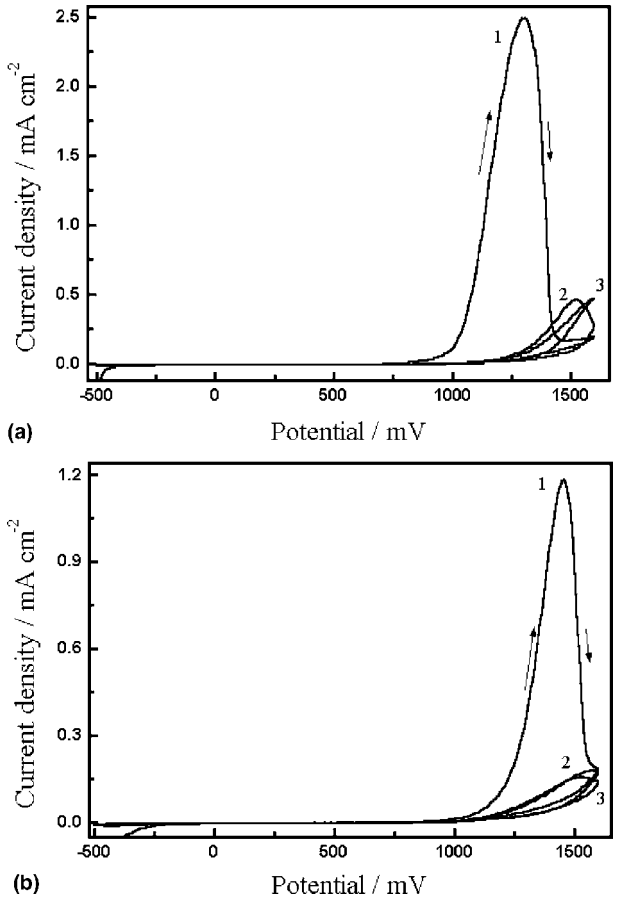

Fig. 1. Cyclic voltammograms of electrodeposition of 0.05 M BT recorded with a Pt electrode in AC, in presence of (a) 0.1 M $LiBF_4$ and (b) 0.1 M $LiCF_3SO_3$.

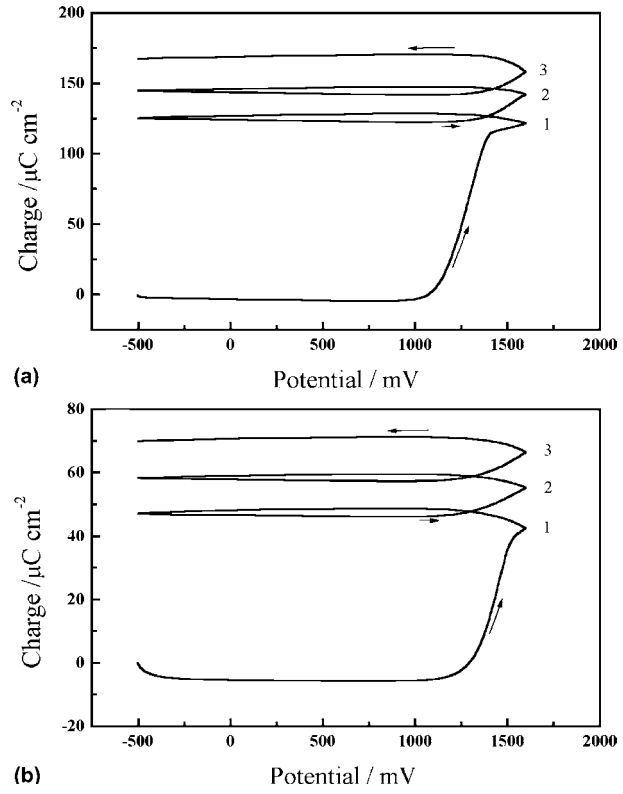

Fig. 2. Charge variation versus potential for electrodeposition of 0.05 M BT recorded with a Pt electrode in AC, in presence of (a) 0.1 M $LiBF_4$ and (b) 0.1 M $LiCF_3SO_3$.

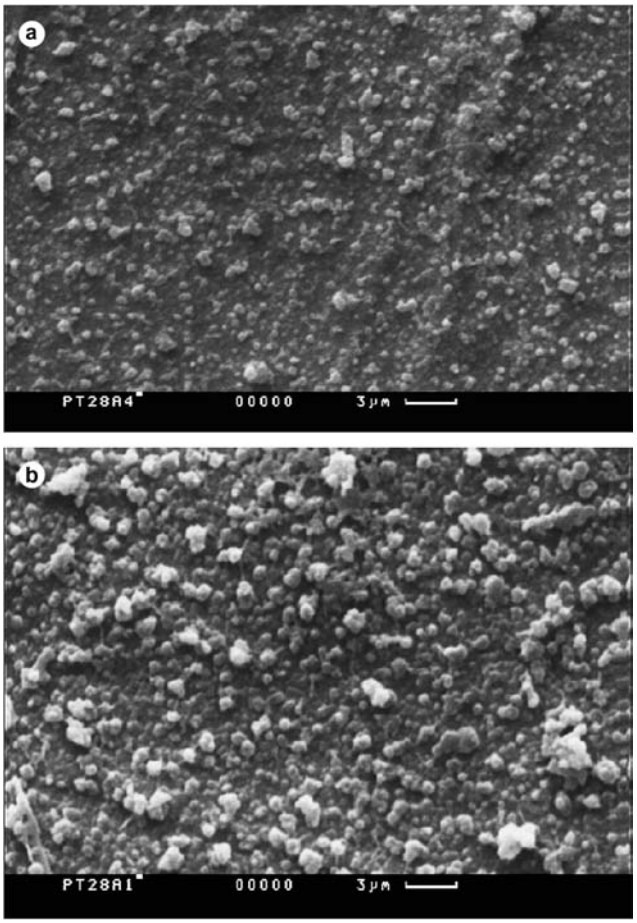

Fig. 3. SEM of (a) PBT/$LiBF_4$ and (b) PBT/$LiCF_3SO_3$ films electrodeposited on platinum electrode.

than 1000 mV, almost no change in Q_c occurs during the oxidation of BT. This means that no polymerization occurs in this range of potential.

The data in Figure 1 show the height of the anodic current peak (1st cycle) decreases with the increase in anion size in the order $BF_4^- > CF_3SO_3^-$. This may be explained by deactivation of PBT film formed in the first cycle. The geometry and softness of these anions BF_4^-, ClO_4^- and $CF_3SO_3^-$ have been regarded as the mean reason for interpreting these results. The $CF_3SO_3^-$ anion is cylindrical (radius 0.26 nm, length 0.28 nm) carrying a highly delocalized charge, and ClO_4^- or BF_4^- are spherical non-coordinating ions [17] (radius 0.23 and 0.24 nm respectively) [18]. The shape and the electronic characteristics of the dopant anion determine the electrochemical behavior and the charge transport within the polymer [19, 20]. It may be concluded that the polarons, which are involved in the electronic conduction, are more localized by $CF_3SO_3^-$ anion and are consequently less mobile than the BF_4^- and ClO_4^- anions. An explanation for the strong bonding of $CF_3SO_3^-$ might be that its size corresponds exactly to the distance between the two thiophene units [21]. On the other hand, the hard and soft acid base concept developed by Pearson [19] offers an interesting interpretation of the polymer doping interactions. The large conjugated polymeric chain with highly delocalized positive charges can be considered as a soft acid. The more fitted dopant should be a soft base, in which charge delocalization can occur. Thus the electron-withdrawing group $-CF_3$ will ensure this effect in the $CF_3SO_3^-$ ion, its base being softer than BF_4^-, where the increase in the radius of the anion leads to a decrease in the base strength [19]. The SEM of PBT/$LiBF_4$ film (Figure 3a) shows a predominantly smooth morphology, with a compact surface. Figure 3b shows the migrograph of PBT/$LiCF_3SO_3$ film, it has rough morphology, larger nodules and a compact surface. This result means that the significant variation in morphology of the PBT films depends on the type of anion. The variation of Q_c with applied potential in Figure 2 (as example) indicates that the Q_c (1st cycle) during electropolymerization decreases with increase in anion size in the order $BF_4^- > CF_3SO_3^-$. This can be interpreted through the deactivation of PBT film as discussed above.

The effect of the cation type used during electropolymerization on the formed PBT is illustrated in Figure 4. On comparing the data obtained in Figure 1 (Li^+) and Figure 4a (Bu_4N^+), it is noted that the anodic current peak values decrease with increasing cation size in the order $Li^+ > Bu_4N^+$. This may be interpreted in terms of deactivation of the PBT film by the bulky cations [22]. The effect of the cation type on Q_c during electropolymerization of BT on Pt is shown in Figure 4a. Comparison between Q_c in the presence of Li^+ (Figure 2) and for Bu_4N^+ (Figure 4b) indicates that Q_c

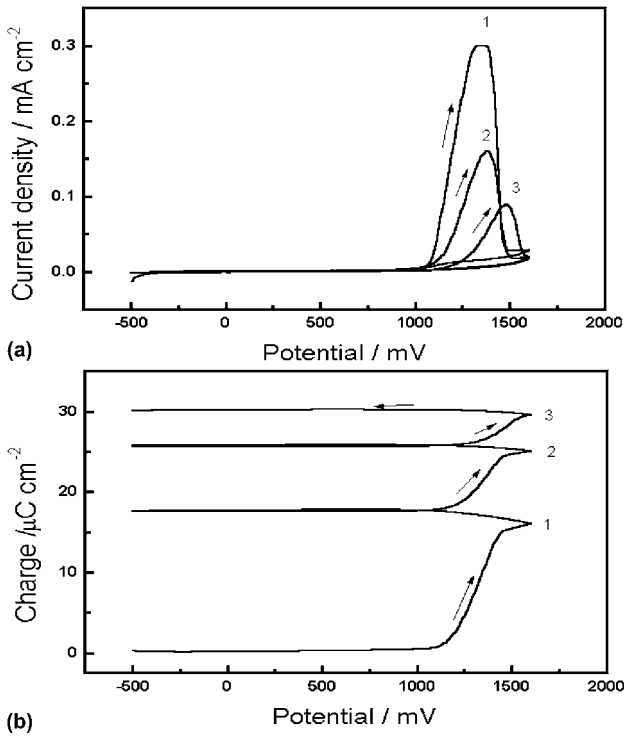

Fig. 4. (a) Cyclic voltammograms and (b) charge variation versus potential of electrodeposition of 0.05 M BT recorded with a Pt electrode in AC, in the presence of 0.1 M Bu_4NBF_4.

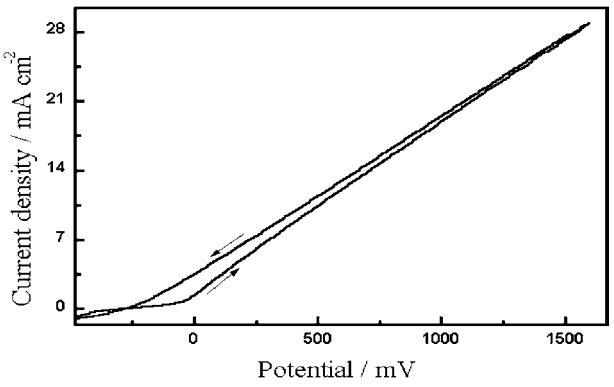

Fig. 5. Cyclic voltammograms for mild steel electrode in AC, in the presence of 0.1 M $LiBF_4$.

decreases with increase in cation size in the order $Li^+ > Bu_4N^+$. This result may be interpreted in terms of deactivation of the PBT film by incorporation of the bulky cations (Bu_4N^+).

3.2. *Electrochemical behavior of mild steel in non-aqueous solution of different electrolytes*

The electrochemical behavior of mild steel was investigating in non-aqueous solution of AC in the presence of the different electrolytes, $LiBF_4$, $LiClO_4$, $LiCF_3SO_3$, Bu_4NBF_4, Bu_4NClO_4, or $Bu_4NCF_3SO_3$. In all cases the steel anode did not exhibit an active/passive transition, but involved passive/transpassive transition as shown in Figure 5 (as example). The lack of an active/dissolution region near the open circuit potential (zero current) is due to spontaneous passivity. The passive/transpassive transition occurs when the potential reaches a certain critical potential (E_{pit}), the passive current suddenly increases steeply, denoting a breakdown of the passive film, initiation and propagation of pitting attack. The E_{pit} value (from −200 to +700 mV) depends on the type of ions used, whereas in non-aqueous solutions, the passive layer formed on the substrate from iron oxide and/or iron hydroxid is not sufficient to protect the steel substrate from pitting corrosion. Similar results were obtained [23] for the dissolution of iron in AC in the presence of supporting electrolyte (Et_4NClO_4). In contrast to aqueous solution, the corrosion of steel is inhibited with by formation of a film consisting of $Fe(OH)_3$, Fe_2O_3 and FeOOH [24].

3.3. *Electropolymerization of 2,2′-bithiophene on steel*

Figure 6a shows the electropolymerization of the BT on steel by cyclic voltammetry (0–2000 mV) from solution containing BT and AC in the presence of different electrolytes, $LiBF_4$, $LiClO_4$, $LiCF_3SO_3$, Bu_4NBF_4, Bu_4NClO_4, and $Bu_4NCF_3SO_3$. No anodic current peak was observed and a linear increase in the current density as a function of applied potential is obtained in the presence of all electrolytes (in 1st cycle). It is clear that the current density decreases with increase in anion size

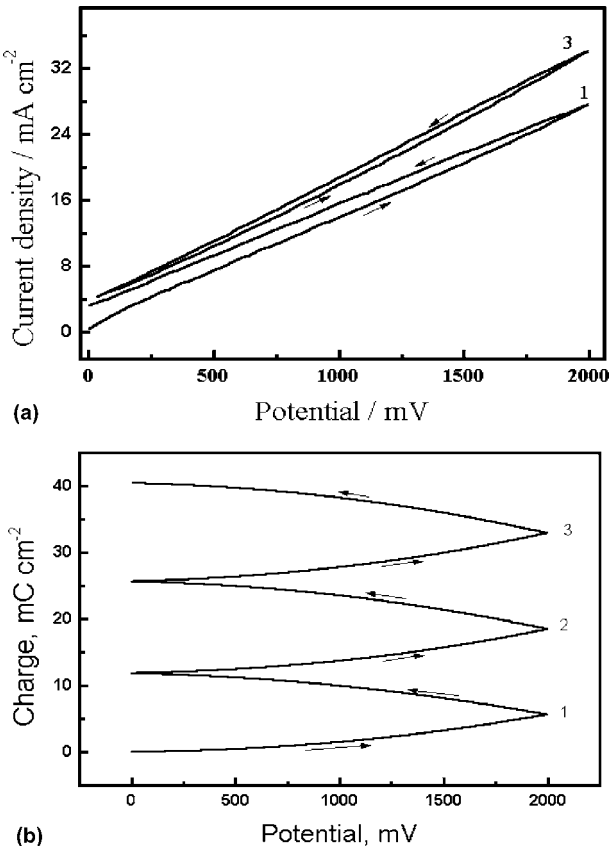

Fig. 6. (a) Cyclic voltammograms and (b) charge variation verses potential of electrodeposition of 0.05 M BT recorded with a steel electrode in AC, in the presence of 0.1 M $LiBF_4$.

in the order: $BF_4^- > CF_3SO_3^-$ and cation size in the order: $Li^+ > Bu_4N^+$. This can be interpreted by the higher mobility of the smaller anions and/or cations in the passive iron oxide layer, which means that the electrochemical and physical properties of the produced PBT film depend on the type of ion used during electropolymerization. On comparing Figure 6a (BT/St) with Figure 1 (BT/Pt), the current density during electropolymerization of BT on steel is higher than that on Pt. By comparing the results obtained in Figure 1 (BT/Pt), 5 (St) and 6a (BT/St), it can be seen that there are two processes taking place in the BT/St system. The first is the dissolution of steel to form iron oxides in the potential range −250 to nearly +700 mV. The second is the deposition of PBT film on the metal oxides and/or base steel surface at potentials >700 mV. Figure 6a indicates that repeated cycling causes an increase in current density with the increase in cycle number. This may be due to the reactivation of PBT film, which is polarized to high potential (>1500 mV) [11]. During experiments, the color of the solution without monomer changed from yellow to orange, probably due to oxidation of the steel substrate with the formation of Fe^{3+} ions [25]. In the presence of BT the solution turned yellow, i.e. the steel dissolution was inhibited as a result of the formation of the PBT film. The color intensity depends on the type of electrolyte used during electro-

polymerization. The color intensity increased with decrease in anion size in the order: $BF_4^- > CF_3SO_3^-$ and the cation size in the order: $Li^+ > Bu_4N^+$. This means that the electrochemical and physical properties of the PBT produced film depend on the type of ion used during electropolymerization. Figure 6b shows the relation between Q_c and applied potential during electropolymerization of BT on steel in the presence of different electrolytes, $LiBF_4$, $LiClO_4$, $LiCF_3SO_3$, Bu_4NBF_4, Bu_4NClO_4, and $Bu_4NCF_3SO_3$. Q_c increases with the increase in potential from 200 mV up to the maximum applied potential (2000 mV). The Q_c (1st cycle) decreased with increase anion size in the order: $BF_4^- > CF_3SO_3^-$ and cation in the order: $Li^+ > Bu_4N^+$.

Figure 6a indicates the effect of the anion type (BF_4^-, ClO_4^- and $CF_3SO_3^-$) on the quality of the PBT film on steel. The anodic current density decreases with increase in anion size. This may be due to deactivation of the PBT film formed by the incorporation of the bulky anions into polymer film (as $CF_3SO_3^-$). It is well known that the oxidation and reduction reactions of PBT film can be controlled by diffusion of the ions into the polymer film [26]. SEM examinations of the steel surface, potentiodynamically polarized from 0 to 2000 mV in the presence of 0.05 M BT and 0.1 M electrolyte, were carried out. The micrographs show that the steel is coated by a thick, non-porous and homogenous film (Figure 7a). This is due to electrodeposition of PBT film on the steel and/or on the passive layer around the pits in the early stages (initiation and propagation). Fe_xO_y–polythiophene and/or FeOOH–polythiophene composite covers the iron surface as elucidated by XPS [27] for the polythiophene–iron system. A similar result was obtained for the polypyrrole–zinc system, where the zinc oxide–polypyrrole composite was formed [28]. SEM indicates that the PBT/$LiCF_3SO_3$ film (Figure 7b) formed on the steel surface is thicker and more compact than the PBT/$LiBF_4$ film. This may be due to the difference in the physical properties of the anions.

The cyclic voltammetry curves for electropolymerization of BT on the steel in the presence of different electrolytes are shown in Figure 8a. Comparison of the anodic current density in the presence of Li^+ (Figure 6a) and Bu_4N^+ (Figure 8a) indicates that the current density decreases with increasing cation size. This may be explained by the difference in cation mobility, their exclusion from the polymer matrix and PBT deactivation due to incorporation of the bulky cations. Similar observations were obtained by Ronclai et al. [29] for polypyrrole. It has been suggested that the anions and cations are incorporated into the polypyrrole film matrix

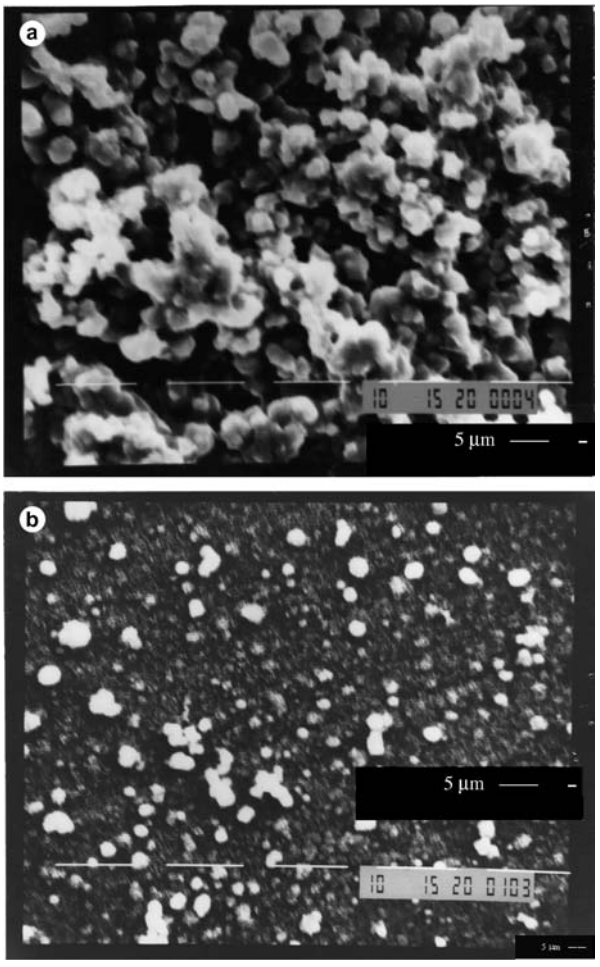

Fig. 7. SEM of (a) PBT/$LiBF_4$ and (b) PBT/$LiCF_3SO_3$ films electrodeposited on steel electrode.

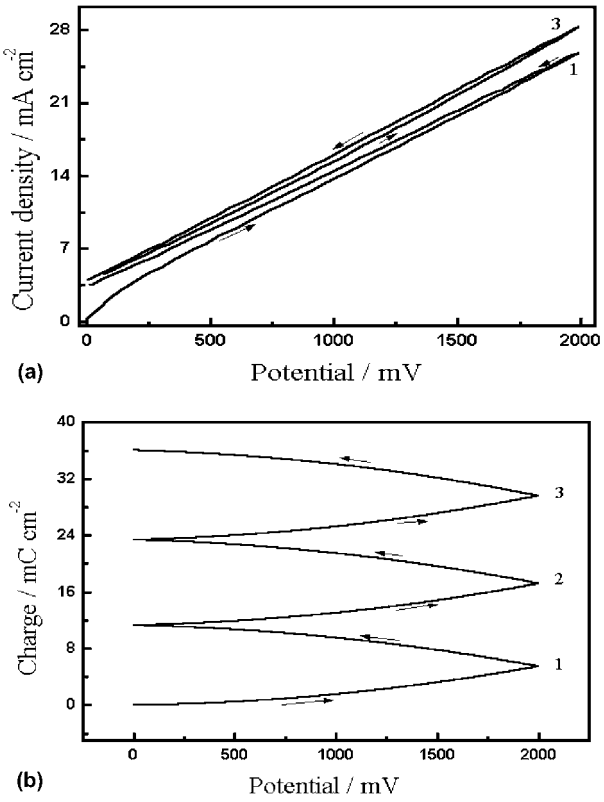

Fig. 8. (a) Cyclic voltammograms and (b) charge variation verses potential cyclic voltammograms of electrodeposition of 0.05 M BT recorded with a mild steel electrode in AC, in the presence of 0.1 M Bu_4NBF_4.

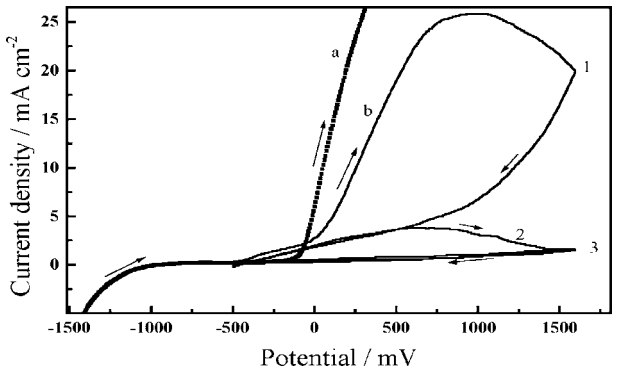

Fig. 9. Anodic behavior of (a) steel and (b) steel coated by PBT film in 0.1 M BT Na_2CO_3 solution containing 0.1 M NaCl. The numbers 1, 2 and 3 denotes to the cycle number.

during the doping process. Q_c variation against potential during PBT electropolymerization on steel in the presence of different electrolytes, Bu_4NBF_4, Bu_4NClO_4, and $Bu_4NCF_3SO_3$, was obtained, as shown in Figure 8b. Comparison of Q_c for the doping cation, Li^+, as indicated in Figure 6b and Bu_4N^+ (Figure 8b), shows that Q_c decreases as cation size increase.

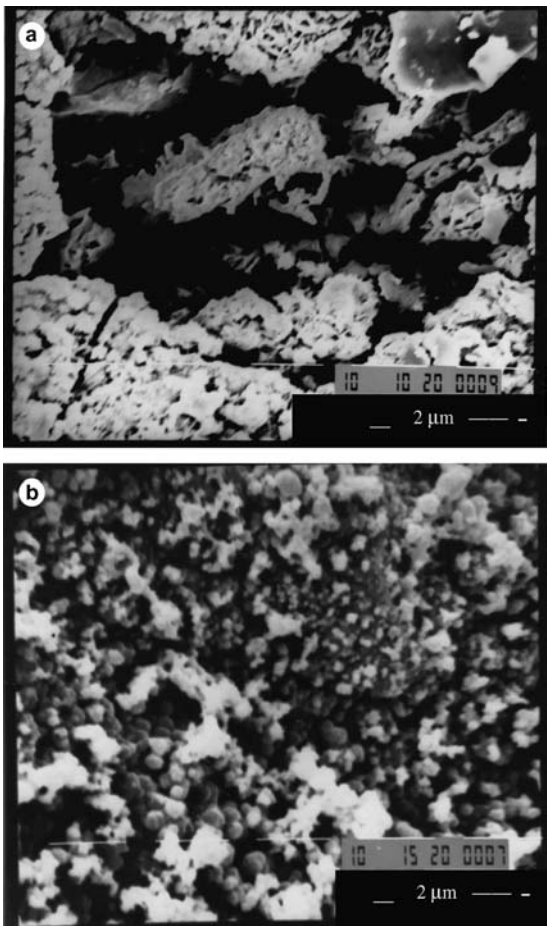

Fig. 10. SEM for (a) steel and (b) steel coated by PBT/$LiCF_3SO_3$ film in 0.1 M Na_2CO_3 solution containing 0.1 M NaCl.

3.4. *Corrosion of steel in aqueous Na_2CO_3 solution containing Cl^- ions*

Figure 9 (curve a) shows the potentiodynamic curve of steel in 0.1 M Na_2CO_3 aqueous solution containing 0.1 M NaCl. No active–passive transition process occurs. Steel has a passive transpassive transition. Initiation of pitting corrosion may be attributed to competitive adsorption between aggressive Cl^- ions and the passivating species (OH^- and H_2O dipoles) [30]. At E_{pit}, Cl^- anions displace the adsorbed passivating species at some locations and accelerate local anodic dissolution. The initiation of pitting corrosion may be due to the ability of Cl^- ions to penetrate the passive film and attack the base metal surface [31]. The pitting growth (propagation) occurs as a result of Cl^- migration inside the pits and hydrolysis of the produced Fe^{2+} ions. SEM indicates that the steel surface has high pit density (Figure 10a).

3.5. *Corrosion of steel coated by PBT in aqueous Na_2CO_3 solution containing Cl^-*

Steel coated by PBT was investigated in 0.1 M Na_2CO_3 solution containing 0.1 M NaCl as shown in Figure 9b. The anions used for the synthesis of PBT films were BF_4^-, ClO_4^- or $CF_3SO_3^-$ and the anions used for investigation of steel coated by PBT films were Cl^- and CO_3^{2-}. The passive current density decreased with increasing cycle number i.e. the passive layer is thicker and less porous. Several authors have attributed the passive current to a capacitive charging current, similar to the behavior of porous metals [20]. The increasing in ion size used during synthesis of PBT leads to a decrease in the passive current. This may be interpreted as due to plugging of these ions in the pits of the passive film, i.e. Cl^- are not able to penetrate through the pits and rupture the passive layer [17]. The ionic radius may be an important parameter; ionic radius increases in the order: $Cl^- < CO_3^{2-} < BF_4^- < ClO_4^- < CF_3SO_3^-$ [32]. It is reasonable to assume that the bigger anions such as BF_4^-, ClO_4^- or $CF_3SO_3^-$ cannot be exchanged from the passive layer by smaller Cl^- anions.

The anodic current peak density (i_{ap}) for the PBT film depends on the type of anion used during synthesis. i_{ap} decreases rapidly with increasing cycle number as a result of PBT overoxidation, which occurrs at 1200 mV [8]. Overoxidation leads to the formation of an insulating layer, which impedes diffusion of the Cl^- ions to the base steel surface. The pitting corrosion potential (E_{pit}) in the 1st anodic curve equals +50 mV. E_{pit} values depend on the type of anion used during electropolymerization, where it increases with the increase in anion size (Table 1). E_{pit} increases in the positive direction as a result of increase in cycle number. In the 3rd anodic curve, no pitting corrosion was observed ($E_{pit} > 1600$ mV), i.e. formation of PBT–iron oxide composite (insulating protective layer) on the steel leads to complete pitting corrosion inhibition. SEM investigations of steel coated by PBT/$LiCF_3SO_3$ after

Table 1. Effect of anion exchange on E_{pit} of steel coated by PBT film in 0.1 M Na_2CO_3 solution containing 0.1 M NaCl

Type of coat	Electrolyte (synthesis)	Anion (analysis)	E_{pit} /(mV) 1st half cycle
Steel	–	CO_3^- + Cl^-	−70
PBT	$LiBF_4$	CO_3^- + Cl^-	50
PBT	$LiClO_4$	CO_3^- + Cl^-	55
PBT	$LiCF_3SO_3$	CO_3^- + Cl^-	80

Table 2. Effect of cation exchange on E_{pit} of steel coated by PBT film in 0.1 M Na_2CO_3 solution containing 0.1 M NaCl

Type of coat	Electrolyte (synthesis)	Cation (analysis)	E_{pit} (mV) 1st half cycle
Steel	–	Na^+	−70
PBT	Bu_4NBF_4	Na^+	85
PBT	Bu_4NclO_4	Na^+	90
PBT	$Bu_4NCF_3SO_3$	Na^+	105

polarization (3 cycles) from −500 to 1600 mV in 0.1 M Na_2CO_3 solutions containing 0.1 M NaCl is shown in Figure 1b. The pits are absent, i.e. there is complete pitting corrosion inhibition. Table 2 indicates the dependence of E_{pit} on the cation type used for the investigation of steel coated by PBT in 0.1 M Na_2CO_3 solution containing 0.1 M NaCl. The cation used for PBT synthesis was Bu_4N^+ and the cation used for the investigation was Na^+. The use of a bigger cation size (Bu_4N^+) in PBT synthesis leads to an increase in E_{pit} towards more positive potentials, i.e. inhibition of pitting. This may be interpreted as due to plugging of the bigger cation size (Bu_4N^+) in the passive layer pits during synthesis and cannot be exchanged by smaller cation size (Na^+) during subsequent investigation.

4. Conclusions

PBT conducting polymer can be used in the formation of passive protective layers on mild steel. PBT/bulky anion and/or bulky cation films improve the passive oxide layer. The passivation of the steel surface is probably achieved by the formation of a Fe_xO_y–PBT composite, which leads to complete pitting corrosion inhibition.

References

1. A.F. Diaz, K.K. Kanazawa and G.P. Gardidni, *J. Chem. Soc., Chem. Commun.* (1979) 635.
2. K. Kaneto, Y. Kohno, K. Yoshino and Y. Inuishi, *J. Chem. Soc., Chem. Commun.* (1983) 382.
3. D.W. DeBerry, *J. Electrochem. Soc.* **132** (1985) 1022.
4. Z. Deng, W.H. Smyrl and H.S. White, *J. Electrochem. Soc.* **136** (1989) 2152.
5. U. Barsch and F. Beck, *Synth. Met.* **55** (1993) 1638.
6. C. Dusemund and G. Schwitzgebel, *Synth. Met.* **55** (1993) 1396.
7. E.M. Genies and J.M. Pernaut, *Synth. Met.* **10** (1984) 117.
8. D. Sazou and C. Georgolios, *J. Electroanal. Chem.* **429** (1997) 81.
9. J. Przyluski, 'Solid State Phenomena', (SCI-Tech Publications Ltd, USA, 1990), p 176.
10. G. Tourillon and F. Garnier, *J. Electrochem. Soc.* **130** (1983) 2042.
11. S.A.M. Refaey and G. Schwitzgebel, *New Polymeric Mater.* **4** (1995) 301.
12. S.A.M. Refaey, *Appl. Surf. Sci.* **157** (2000) 199.
13. S.A.M. Refaey, S.S. Abd El-Rehim, F. Taha, M.B. Saleh and R.A. Ahamed, *Appl. Surf. Sci.* **158** (2000) 190.
14. M.A. Dury, R.J. Seymour and S.K. Tripathy, in T. Davidson (Ed.), 'ACS Symposium Series No. 242', (1984), p. 473.
15. A.J. Downard and D. Pletcher, *J. Elecroanal. Chem.* **206** (1986) 147.
16. H. Harada, T. Fuchigami and T. Nonaka, *J. Electroanal. Chem.* **303** (1991) 139.
17. R.L. Kay, B.J. Hales and G.P. Cuningham, *J. Phys. Chem.* **71** (1967) 3925.
18. K.B. Jazimirski, Thermochemie von Komplexverbindungen (1956) 40.
19. R.G. Pearson, 'Hard and Soft Acids and Bases', (Dowden, Hutcinson, and Ross, London, 1973), p. 73, 76.
20. F. Garnier, G. Tourillon, J.Y. Barraud and H. Dexpert, *J. Mater. Sci.* **20**. (1985) 2687.
21. G. Tourillon, 'Handbook of Conducting Polymers', Vol. 1 Marcel Dekker, (New York, 1986), Chapter 9.
22. S.A.M. Refaey, G. Schwitzgebel and O. Schneider, *Synth. Met.* **98** (1999) 183.
23. V.L. Shirokii, A.N. Ryabtsev, A.S. Stromsku, N.A. Maier, Yu. A. Oldekop and A.P. Tomilov, *Vestsi. Akad. Navuk. BSSR, Ser. Khim. Navuk* **2** (1988) 117.
24. J. Jha Lakhan and G. Singh, *Trans. SAEST* **25** (1990) 90.
25. A. De Bruyne, PhD thesis, Universite Libre de Bruxelles (1996).
26. G. Tourillon and F. Garnier, *J. Polym. Sci., Polym. Phys.* **22** (1984) 33.
27. S. Aieyach, A. Kone, M. Dieng, J. Aaron and P. Lacaze, *J. Chem. Soc. Chem. Commun.* (1991) 822.
28. M. Bazzaouia, E.A. Bazzaouib, L. Martinsc and J.I. Martinsa, Synth. Met. **128** (2002) 103.
29. J. Roncali, F. Garnier, M. Lemaire and R. Garreau, *Synth. Met.* **15** (1986) 323.
30. T.B. Hoar, D. Mears and G. Rothwell, *Corros. Sci.* **5** (1965) 279.
31. D.C.W. Kannagara and B.E. Conway, *J. Electrochem. Soc.* **134** (1987) 894.
32. Y. Marcus 'Ion Solvation' (John Wiley, 1983), p. 100.